Coulomb excitation 2022Sp01

History

Type	Author	Citation	Literature Cutoff Date
Full Evaluation	Balraj Singh, M. S. Basunia, Jun Chen et al. ,	NDS 192,315 (2023)	25-Sep-2023

Dataset by Balraj Singh, S. Basunia, and IAEA-ICTP workshop participants: S. Das and A. Karmakar.
Beam=^{222}Rn. Targets=^{120}Sn and ^{60}Ni of 2.1 mg/cm^2 thickness.

2022Sp01 (also 2020Bu20,2019Bu29): E(^{222}Rn)=4.23 MeV/nucleon produced in bombardment of thorium carbide with 1.4-GeV protons from CERN PS Booster, followed by separation of ions of interest according to A/Q, and delivered to a Penning trap, REXTRAP, where the singly-charged ions were accumulated and cooled before being allowed into an electron beam ion source, REXEBIS. The ions were then confined in a high-density electron beam that stripped more electrons to produce a charge state of 51$^+$ for ^{222}Rn beam, extracted as 1 ms pulses before being mass-selected again according to A/Q, and injected into the HIE-ISOLDE linear post-accelerator. Measured Eγ, Iγ, $\gamma\gamma$-coin using Miniball array of eight triple-cluster HPGe detectors, each with sixfold segmentation. Scattered particles and recoiling target recoils were detected using a highly segmented silicon ‘CD’ detector with four double-sided silicon strip detectors with 16 annular strips on the front face and 24 radial sectors. Deduced levels, J^π, E2, E3 and E1 matrix elements, and intrinsic dipole, quadrupole and octupole moments, and g.s. and octupole bands. Authors of 2020Bu20 conclude that while octupole vibrations exist, but with no static pear-shapes (or static octupole deformation) in the ground state. Comparison of measured intrinsic electric-octupole moments with theoretical calculations using 2-D Gogny D1S force, QOCH with relativistic PC-PK1 EDF (RMF), covariant density EDF (CDFT), and spdf-IBM-2.

All data are from 2022Sp01.

^{222}Rn Levels

Matrix elements (M.E.) were deduced by 2022Sp01 from measured γ-ray yields with least-squared fit of a total of 89 data points to GOSIA analysis code, using known γ-ray branching ratios of low-lying negative-parity states from earlier studies of ^{222}Rn structure. The matrix elements are in units of eb$^{1/2}$ for E1, eb for E2, and eb$^{3/2}$ for E3.

E(level)[†]	J^π[@]	$T_{1/2}$[&]	Comments
0[a]	0$^+$		
186[a]	2$^+$		Q=−1.4 *+5−6* Q: deduced by evaluators from Diagonal E2 M.E. Diagonal E2 M.E. (186,2$^+$ → 186,2$^+$)=−1.8 *+6−9*. Intrinsic electric quadrupole moment, Q_0=4.8 eb *+24−16*.
448[a]	4$^+$	52.5 ps *+44−23*	E2 M.E. (186,2$^+$ → 448,4$^+$)=+2.55 *+6−10*. Deduced B(E2)↑(186,2$^+$ → 448,4$^+$)=1.30 *+6−10* (evaluators). Intrinsic electric quadrupole moment, Q_0=5.04 eb *+13−20*. For $T_{1/2}$, Eγ=262.27 keV from the Adopted dataset is used.
601[b]	1$^-$	0.7 ps *+11−5*	E1 M.E. (0,0$^+$ → 601,1$^-$)=−0.007 *+3−7* or +0.007 *+7−3*. Deduced B(E1)↑(0,0$^+$ → 601,1$^-$)=0.00005 *+15−3* (evaluators). Intrinsic electric dipole moment, D_0=0.014 eb$^{1/2}$ *+14−6* or −0.014 eb$^{1/2}$ *+6−14*. E3 M.E. (186,2$^+$ → 601,1$^-$)=+0.5 *+2−4*. Intrinsic electric octupole moment, O_0=1.20 eb$^{3/2}$ *+50−90*. E3 M.E. (448,4$^+$ → 601,1$^-$)<1.4. Intrinsic electric octupole moment, O_0<2.90 eb$^{3/2}$. $T_{1/2}$: deduced by evaluators from B(E1)↑ for 601-keV transition and branching ratio of 0.62 for this transition from the Adopted dataset.
636[b]	3$^-$	≈0.4 ns	E2 M.E. (601,1$^-$ → 636,3$^-$)=+2.1 *4*. Intrinsic electric quadrupole moment, Q_0=5.0 eb *10*. Deduced B(E2)↑(601,1$^-$ → 636,3$^-$)=1.5 *+6−5* (evaluators). E3 M.E. (0,0$^+$ → 636,3$^-$)=+0.88 *+11−8*. Intrinsic electric octupole moment, O_0=2.36 eb$^{3/2}$ *+30−21*. E3 M.E. (186,2$^+$ → 636,3$^-$)<1.5. Intrinsic electric octupole moment, O_0<3.50 eb$^{3/2}$. $T_{1/2}$: deduced by evaluators from B(E2)↑ for 34.8-keV transition and branching ratio of

Continued on next page (footnotes at end of table)

Coulomb excitation 2022Sp01 (continued)

^{222}Rn Levels (continued)

E(level)[†]	J^{π}[@]	$T_{1/2}$[&]	Comments
			≈0.3 for this transition from the Adopted dataset.
769[a]	6^+	15.9 ps *+18−11*	E2 M.E. (448,4^+ → 769,6^+)=+3.52 *+13−18*. Deduced B(E2)↑(448,4^+ → 769,6^+)=1.38 *+10−14* (evaluators). Intrinsic electric quadrupole moment, Q_0=5.50 eb *+20−30*.
798[b]	5^-		E2 M.E. (636,3^- → 798,5^-)=+2.7 *7*. Intrinsic electric quadrupole moment, Q_0=4.7 eb *12*. Deduced B(E2)↑(636,3^- → 798,5^-)=0.058 *+15−22* (evaluators). E3 matrix element (from 186, 2^+)=+1.3 *+2−3*. Intrinsic electric octupole moment, O_0=2.30 eb$^{3/2}$ *+30−50*.
867[c]	(2^+)		E2 M.E. (0,0^+ → 867,(2^+))=+0.24 *+3−5*. Intrinsic electric quadrupole moment, Q_0=0.76 eb *+10−16*. Deduced B(E2)↑(0,0^+ → 867,(2^+))=0.058 *+15−22* (evaluators). E2 M.E. (186,2^+ → 867,(2^+))=+0.52 *+14−20*. Deduced B(E2)↑(186,2^+ → 867,(2^+))=0.054 *33* (evaluators). Intrinsic electric quadrupole moment, Q_0=1.40 eb *+40−50*.
867[d]	(0^+)		E1 M.E. (601,1^- → 867,(0^+))=0.0057 *20*. Deduced B(E1)↑(601,1^- → 867,(0^+))=0.000011 *+9−6* (evaluators). Intrinsic electric dipole moment, D_0=0.012 eb$^{1/2}$ *4*. E2 M.E. (186,2^+ → 867,(0^+))=+0.32 *5*. Deduced B(E2)↑(186,2^+ → 867,(0^+))=0.021 *6* (evaluators). Intrinsic electric quadrupole moment, Q_0=1.01 eb *16*.
959[c]	(3^+)		E2 M.E. (186,2^+ → 959,(3^+))=−1.2 *+19−3*. Deduced B(E2)↑(186,2^+ → 959,(3^+))=0.29 *+16−19* (evaluators). Intrinsic electric quadrupole moment, Q_0=2.0 eb *+10−40*.
1049[b]	7^-		E2 M.E. (798,5^- → 1049,7^-)=+4.0 *9*. Deduced B(E2)↑(798,5^- → 1049,7^-)=1.5 *+7−6* (evaluators). Intrinsic electric quadrupole moment, Q_0=5.8 eb *13*.
1053?[#d]	(2^+)		
1111[c]	(4^+)		E2 M.E. (448,4^+ → 1111,(4^+))=+0.91 *+14−20*. Deduced B(E2)↑(448,4^+ → 1111,(4^+))=0.092 *+31−36* (evaluators). Intrinsic electric quadrupole moment, Q_0=1.60 eb *+30−40*.
1128[a]	8^+	7.3 ps *+11−16*	E2 M.E. (769,6^+ → 1128,8^+)=+4.5 *+6−3*. Deduced B(E2)↑(769,6^+ → 1128,8^+)=1.56 *+44−20* (evaluators). Intrinsic electric quadrupole moment, Q_0=6.00 eb *+80−40*.
1315?[#d]	(4^+)		
1319?[#c]	(5^+)		
1357[b]	9^-	7 ps *+9−5*	$T_{1/2}$: from B(E2)↑ for 308γ, and branching from the Adopted dataset. E2 M.E. (1049,7^- → 1357,9^-)=+5.5 *+21−13*. Deduced B(E2)↑(1049,7^- → 1357,9^-)=2.0 *+19−8* (evaluators). Intrinsic electric quadrupole moment, Q_0=7.0 eb *+30−20*.
1513[a]	10^+	7.8 ps *+51−12*	E2 M.E. (1128,8^+ → 1513,10^+)=+4.1 *+5−9*. Deduced B(E2)↑(1128,8^+ → 1513,10^+)=0.99 *+26−39* (evaluators). Intrinsic electric quadrupole moment, Q_0=4.9 eb *+7−11*.
1575?[#c]	(6^+)		
1637?[#d]	(6^+)		
1708[‡b]	11^-		
1877?[#c]	(7^+)		
1913[‡a]	12^+		
2089[‡b]	13^-		
2219?[#c]	(8^+)		

Continued on next page (footnotes at end of table)

Coulomb excitation 2022Sp01 (continued)

^{222}Rn Levels (continued)

E(level)[†]	J^{π}[@]
2317[‡a]	14^+
2485[‡b]	15^-

[†] From 2022Sp01, based on their Eγ data, unless stated otherwise.
[‡] Level included in the GOSIA analysis based on a level observed in ^{232}Th(^{136}Xe,Xγ) (1999Co02), but not observed in the present experiment, thus not included in the Adopted Levels.
[#] Level included in the GOSIA analysis based on J(J+1) extrapolation, not observed in the present experiment, thus not included in the Adopted Levels.
[@] As proposed by 2022Sp01, based on population of an even-even nucleus in Coulomb excitation process with E2 excitations, and band structures.
[&] Deduced by evaluators from B(E2)↑ values from E2 matrix elements measured in the present work.
[a] Band(A): g.s. band.
[b] Band(B): Octupole band based on 1^-. Average magnitude of D_0/Q_0=0.00021 fm^{-1} *3* (1997Co08); D_0=0.10 efm *2* (1997Co14).
[c] Band(C): Tentative γ band.
[d] Band(D): Tentative β band.

γ(^{222}Rn)

B(E2)(W.u.) values deduced by evaluators from the measured E2 matrix elements in the present work.

E_γ[†]	E_i(level)	J_i^π	E_f	J_f^π	Mult.	α[‡]	Comments
(34.8)	636	3^-	601	1^-	[E2]	1.30×10^3 *4*	B(E2)(W.u.)=80 *+32−27* I(γ+ce)(34.8)/I(γ+ce)(449)=≈42/≈100 (from the Adopted dataset).
163.0[@] *5*	798	5^-	636	3^-	[E2]	1.116 *21*	B(E2)(W.u.)=4.6 *+12−17* E_γ: from the Adopted dataset.
186	186	2^+	0	0^+	E2	0.677 *9*	Mult.: from the Adopted Gammas, also Coulomb excited from 0^+ in the present study.
229	1357	9^-	1128	8^+	[E1]	0.0624 *9*	Iγ(229)/Iγ(308)=74 *42*/100 *42* (from the Adopted dataset).
251	1049	7^-	798	5^-			B(E2)(W.u.)=26×10^1 *+12−10*
262	448	4^+	186	2^+	[E2]	0.2093 *29*	B(E2)(W.u.)=90 *+4−7* α: for Eγ=262.27 *5* from the Adopted dataset.
266 *2*	867	(0^+)	601	1^-	[E1]	0.0438 *10*	B(E1)(W.u.)=1.4×10^{-3} *+11−8*
281	1049	7^-	769	6^+			
308	1357	9^-	1049	7^-	[E2]	0.1279 *19*	B(E2)(W.u.)=20×10^1 *+19−8*
320	769	6^+	448	4^+	[E2]	0.1144 *16*	B(E2)(W.u.)=120 *+9−12* α: for Eγ=319.6 *2* from the Adopted dataset.
349	798	5^-	448	4^+			
360	1128	8^+	769	6^+	[E2]	0.0819 *12*	B(E2)(W.u.)=149 *+42−19* α: for Eγ=359.6 *2* from the Adopted dataset.
385	1513	10^+	1128	8^+	[E2]	0.0680 *10*	B(E2)(W.u.)=100 *+26−39* α: for Eγ=384.9 *2* from the Adopted dataset.
415	601	1^-	186	2^+	[E1]	0.0163 *2*	Iγ(415)/Iγ(601)=60/100 (from the Adopted dataset).
449	636	3^-	186	2^+	[E1]	0.0137 *2*	
601	601	1^-	0	0^+	[E1]	0.0076 *1*	B(E1)(W.u.)=7×10^{-4} *+21−4*
663	1111	(4^+)	448	4^+			B(E2)(W.u.)=11.5 *+39−45*
681[#]	867	(2^+)	186	2^+	[E2+M1]	0.042 *25*	B(E2)(W.u.)=6.8 *42*
681[#]	867	(0^+)	186	2^+	[E2]	0.0176 *3*	B(E2)(W.u.)=13 *4*

Continued on next page (footnotes at end of table)

Coulomb excitation 2022Sp01 (continued)

$\gamma(^{222}Rn)$ (continued)

E_γ †	E_i(level)	J^π_i	E_f	J^π_f	Mult.	α ‡	Comments
							Iγ(681γ)/Iγ(266γ)=1.9 +*38*−*12*, deduced by evaluators from B(E2)(W.u.)/B(E1)(W.u.) ratio.
773	959	(3$^+$)	186	2$^+$			B(E2)(W.u.)=26 +*14*−*17*
867	867	(2$^+$)	0	0$^+$	[E2]	0.0107 *2*	B(E2)(W.u.)=1.5 +*4*−*5* Iγ(867γ)/Iγ(681γ)=0.7 +*6*−*4*, deduced by evaluators from B(E2)(W.u.) ratio, assuming 681 is pure E2.

† From 2022Sp01.

‡ Total theoretical internal conversion coefficients, calculated using the BrIcc code (2008Ki07) with Frozen orbital approximation based on γ-ray energies, assigned multipolarities, and mixing ratios, unless otherwise specified.

Multiply placed.

@ Placement of transition in the level scheme is uncertain.

Coulomb excitation 2022Sp01

Level Scheme

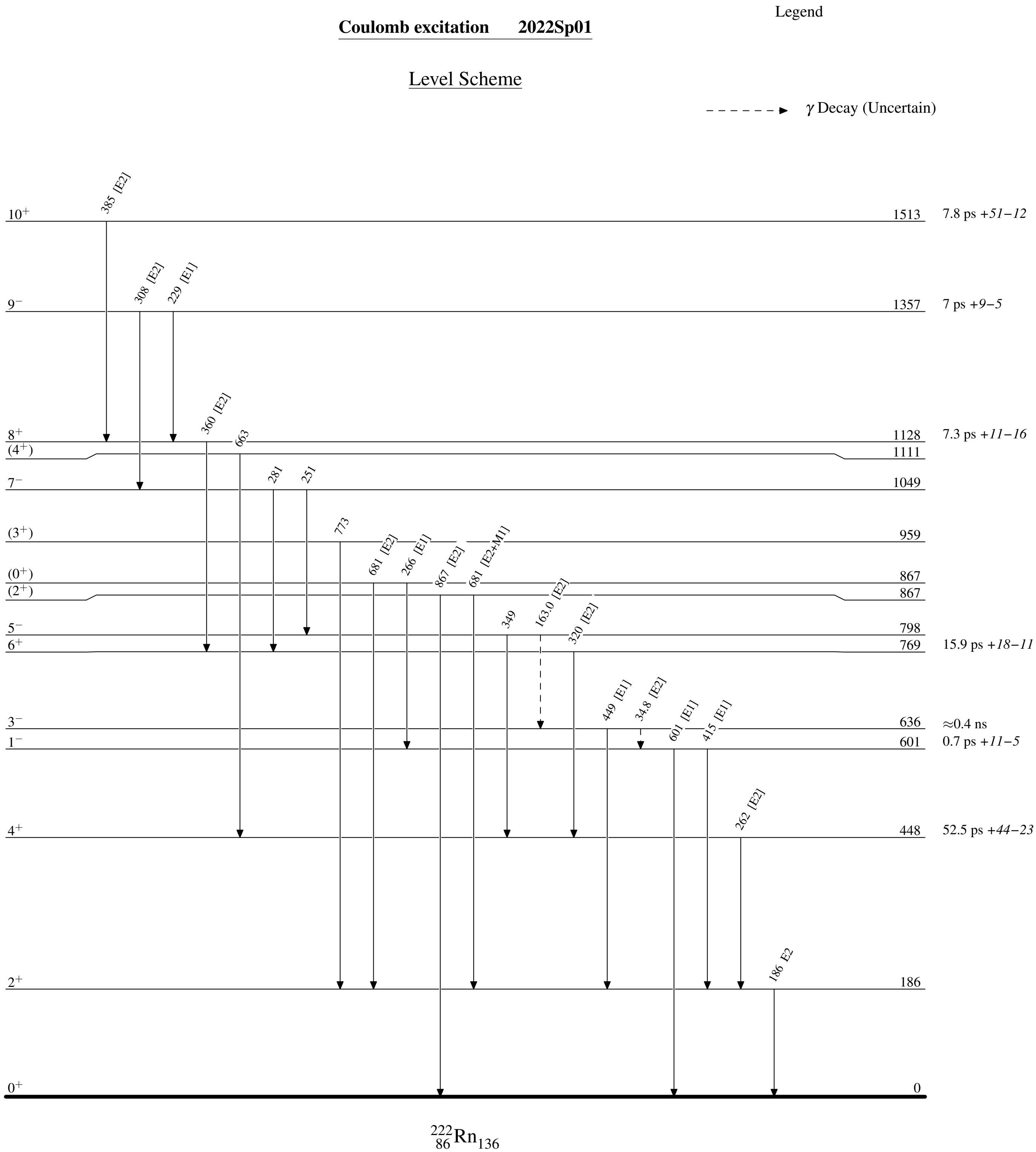

Coulomb excitation 2022Sp01

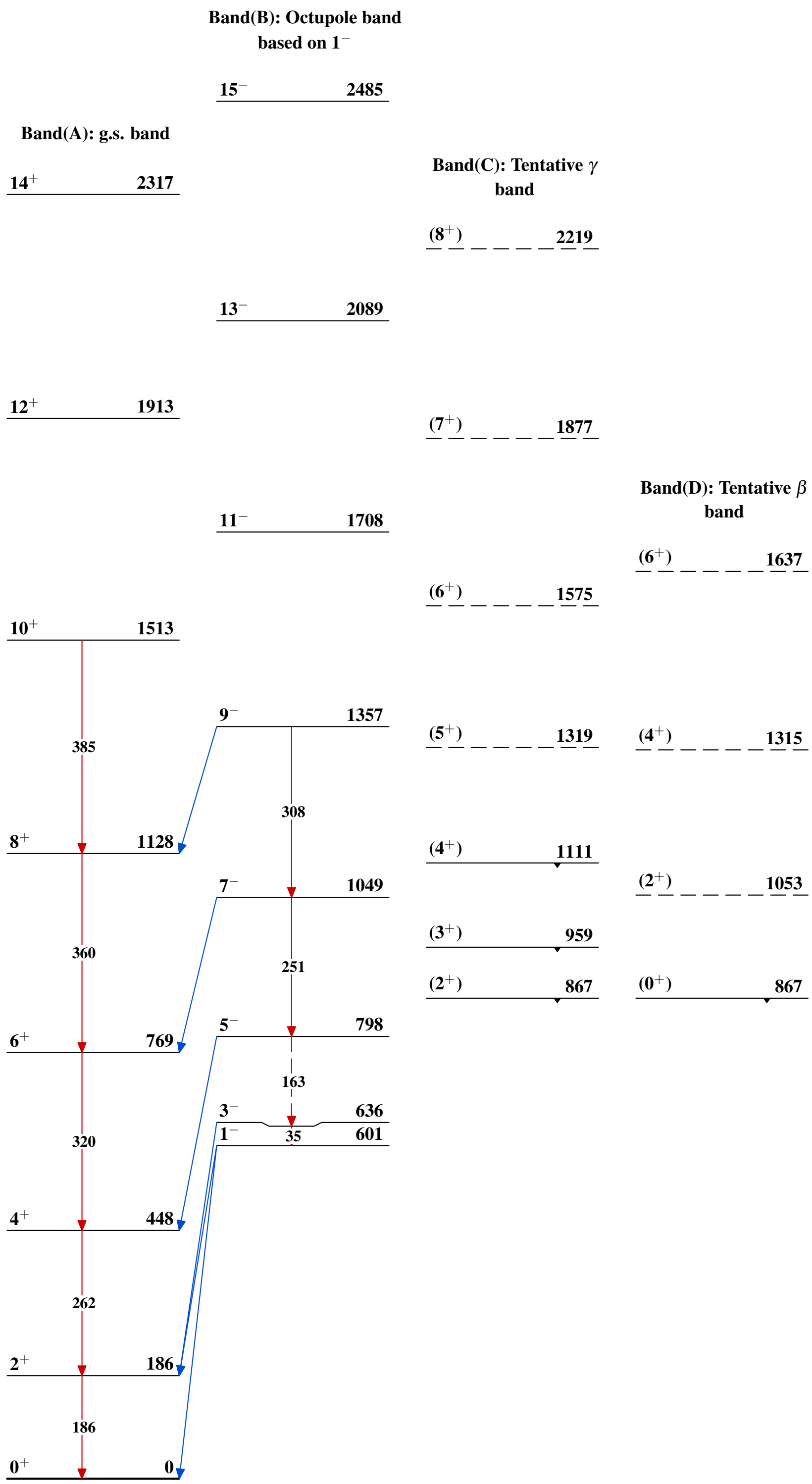

$^{222}_{86}Rn_{136}$